CHEMMEDCHEM

CHEMISTRY ENABLING DRUG DISCOVERY

Accepted Article

Title: N-Benzyl substitution of polyhydroxypyrrolidines - the way to selective inhibitors of Golgi α-mannosidase II

Authors: Sergej Šesták, Maroš Bella, Tomáš Klunda, Soňa Gurská, Petr Džubák, Florian Wöls, Iain BH Wilson, Vladimir Sladek, Marián Hajdúch, Monika Polakova, and Juraj Kóňa

To be cited as: *ChemMedChem* 10.1002/cmdc.201700607

Link to VoR: http://dx.doi.org/10.1002/cmdc.201700607

A Journal of

ChemPubSoc Europe

WILEY-VCH

www.chemmedchem.org

N-Benzyl substitution of polyhydroxypyrrolidines - the way to selective inhibitors of Golgi α-mannosidase II

Sergej Šesták, [a] Maroš Bella, [a] Tomáš Klunda, [a] Soňa Gurská, [b] Petr Džubák, [b] Florian Wöls, [c] Iain B. H. Wilson, [c] Vladimir Sladek, [a] Marián Hajdúch, [b] Monika Poláková,*[a] Juraj Kóňa*[a]

[a] Dr. Sergej Šesták, Dr. Maroš Bella, Tomáš Klunda, Dr. Vladimir Sladek, Dr. Monika Poláková, Dr. Juraj Kóňa
Institute of Chemistry, Center for Glycomics
Slovak Academy of Sciences
Dúbravská cesta 9, 845 38 Bratislava, Slovakia
E-mail: monika.polakova@savba.sk (M. Poláková), juraj.kona@savba.sk (J. Kóňa)
[b] Dr. Soňa Gurská, Dr. Petr Džubák, Assoc. Prof. Marián Hajdúch
Laboratory of Experimental Medicine, Institute of Molecular and Translational Medicine, Faculty of Medicine and Dentistry
Palacky University and University Hospital in Olomouc
Puškinova 6, 775 20 Olomouc, Czech Republic
[c] Florian Wöls, Dr. Iain B. H. Wilson
Department of Chemistry
University of Natural Resources and Life Sciences
A-1190 Vienna, Austria

Supporting information for this article is given via a link at the end of the document. It contains experimental procedures and analytical data for compounds **2** - **22**, and calculated FMO-PIEDA interaction energies between the inhibitors and active-site amino acids of dGMII.

Abstract: Inhibition of biosynthesis of complex *N*-glycans in Golgi apparatus influence progress of tumor growth and metastasis. Golgi α-mannosidase II (GMII) has become a therapeutic target for a drug with anticancer activities. One critical task for successful application GMII drugs in medicine treatment is to reduce their unwanted co-inhibition with lysosomal α-mannosidase (LMan) by which suffer all known potent GMII inhibitors. A series of novel *N*-substituted polyhydroxypyrrolidines was synthesized and tested with modeled GH38 α-mannosidases from *Drosophila melanogaster* (GMIIb and LManII). The most potent structures inhibited GMIIb (K_i = 50-76 μM as determined by enzyme assays) with a significant selectivity index of IC_{50}(LManII)/IC_{50}(GMIIb) > 100. They also showed the inhibitory activity in vitro assays with MTS test towards cancer cell lines (leukemia, IC_{50} = 92-200 μM) and low cytotoxic activity towards normal fibroblast cell lines (IC_{50} > 200 μM). In addition, they did not show any significant inhibitory activity towards GH47 *Aspergillus saitoi* α1,2-mannosidase. An appropriate stereo configuration of -CH_2OH and benzyl functional groups on the pyrrolidine ring of the inhibitor may lead to an inhibitor with the required selectivity to the active site of a target α-mannosidase.

Introduction

Swainsonine **1** [(1*S*,2*R*,8*R*,8a*R*)-trihydroxy-indolizidine] is an alkaloid naturally occurring in a number of Australian and North American plants.[1] It was found that it interferes with the glycosylation pathway where it specifically inhibits glycoside hydrolases from the GH family 38.[2] Swainsonine has attracted attention as a potential anticancer agent as it inhibits tumor growth and metastasis, augments natural killer and macrophage-mediated tumor cell killing, and stimulates bone marrow cell proliferation.[2g, 3] The effect of swainsonine on oligosaccharide processing was elucidated [2b, 2d, 2f, 4] as it binds reversibly to the active site of Golgi α-mannosidase II (GMII) (EC 3.2.1.114)[5] and modulates *N*-glycoprotein synthesis resulting in the accumulation of hybrid type of *N*-glycans.[2e, 6] Clinical trials of short duration have demonstrated that swainsonine has a low toxicity in humans and is well tolerated.[2g, 7] On the other hand, swainsonine and all other known α-mannosidase inhibitors have an additional serious side effect that potentially precludes their use as therapeutics. These compounds also inhibit the broad-specificity lysosomal α-mannosidase (LMan) (EC 3.2.1.24, GH family 38)[8] resulting in the accumulation of mannose-containing oligosaccharides in tissues, serum and urine.[2g, 4]

To apply swainsonine-mechanism-based compounds as therapeutics, selective inhibitors of GMII with minimized side effect to LMan are required. However, the potent inhibitors of GMII exhibited negligible or no selectivity.[5a, 5f, 9] It was observed that 3- and 5-substituted swainsonine derivatives exhibited a weak selectivity towards GMII [IC_{50}(LMan)/IC_{50}(GMII) < 20] at the nanomolar and micromolar levels, while 6- and 7-substituted derivatives exhibited even poorer activity and selectivity at the micromolar and millimolar levels.[5f, 10] Some polyhydroxypyrrolidine derivatives also showed weak selectivity.[9a, 9b]

The active site of *Drosophila melanogaster* Golgi α-mannosidase II (dGMII) is made up of three sugar-binding sites: the catalytic, holding, and anchor subsites.[5a, 5b, 11] dGMII needs Zn^{2+} ion co-factor for catalytic activity which resides at the bottom of the catalytic subsite.[5b] Zn^{2+} ion is in octahedral coordination with four amino acid residues (side chains of His90, Asp92, Asp204, His471) and with an inhibitor (bidentate ligand). All potent dGMII inhibitors have to bind properly to the bottom of the active site by interaction with Zn^{2+} and neighboring amino acid residues otherwise the potency of the inhibitor is dropped dramatically.[9a, 9b, 9e, 9f, 9i-k, 10c, 12] The critical role of Zn^{2+} ion and aspartic acid residues of the catalytic subsite for the interactions with the dGMII inhibitors was recently confirmed by quantum mechanics calculations.[13] From crystal structures of available fruit fly dGMII[5b, 11a] and bovine bLMan[8a] it is evident that the active site of both enzymes are structurally and chemically almost identical in radius of 10 Å around Zn^{2+} ion co-factor. This is one of reasons why structurally small potent GMII inhibitors like swainsonine inhibit both enzymes effectively with no

significant selectivity observed. Thus, our strategy in the design of a selective GMII inhibitor was based on a previous proposal,[5a, 12c] and consists of two basic points: (i) design of the core unit of the inhibitor (key interactions with catalytic subsite which is identical in both dGMII and bLMan); and (ii) design of structural linker (specific interactions with holding or anchor subsites of dGMII which are missing in bLMan).[5a, 8a, 11a] For these purposes, polyhydroxypyrrolidines with *N*-substitution were prepared. It is known that certain polyhydroxypyrrolidines derived from natural 1,4-dideoxy-1,4-imino-D-mannitol (the structure **24**), an azafuranose analogue of mannose, are inhibitors of both GMII and LMan at the micromolar or millimolar level with a weak selectivity index to GMII observed for some *N*-substituted derivatives [9a, 9b] (for more details about the design of the structure of the inhibitors see the section Molecular modeling). Our research group has recently published a series of articles with mannose derivatives to find a structural feature of the inhibitor with impact on selectivity.[9p-r] These studies revealed that a selective GMII inhibitor should have a linker of the benzyl type and modified 6-OH functional group. Structural design was further developed and the present paper reports a study with six novel *N*-arylalkyl substituted pyrrolidines from which, to the best of our knowledge, some of them are the first GH38 inhibitors with a significant selectivity index of IC_{50}(LManII)/IC_{50}(GMIIb) > 100 (for more details on the modeled GH38 enzymes, LManII and GMIIb, see the section Enzyme assays – experimental).

Results and Discussion

In the following subsections, the results from synthesis, biological assays and molecular modeling are described and discussed in connection with the selected Golgi and lysosomal enzymes from the GH family 38 which are abbreviated as follows: GMII (human Golgi α-mannosidase II),[9a, 9b] dGMII (fruit fly Golgi α-mannosidase II, the homologue of mammalian Golgi α-mannosidase II),[5b, 14] GMIIb (fruit fly Golgi α-mannosidase II with some distinct differences in comparison to other invertebrates and vertebrates),[15] LMan (human lysosomal α-mannosidase),[8b, 9a, 9b] dLMan (fruit fly lysosomal α-mannosidase, CG6206 gene product),[5f] LManII (fruit fly lysosomal α-mannosidase, one of the acidic class II mannosidases),[15] JBMan (Jack bean α-mannosidase, the plant homologue of the acidic class II mannosidases)[16] and bLMan (bovine lysosomal α-mannosidase).[8a] The fruit fly GMIIb, LManII and JBMan were used for enzymatic assays in this study and our previous studies;[9p-r] GMII, dGMII, LMan, dGMII and JBMan in other previous studies,[5f, 9a-o] while dGMII and bLMan are the enzymes with available crystal structures.[5a, 5b, 8a, 12c, 17]

Synthesis

Computer-assisted design[18] was used to predict a core structure and a selectivity structural linker of the dGMII inhibitor (for more details see also the section Molecular modeling). The synthesis of target compounds started from 2,3-*O*-isopropylidene derivatives **2** and **3** which were prepared from D-ribose according to the previously published procedure (Scheme 1).[19]

Highly efficient reductive ring opening of the lactols **2** and **3** with

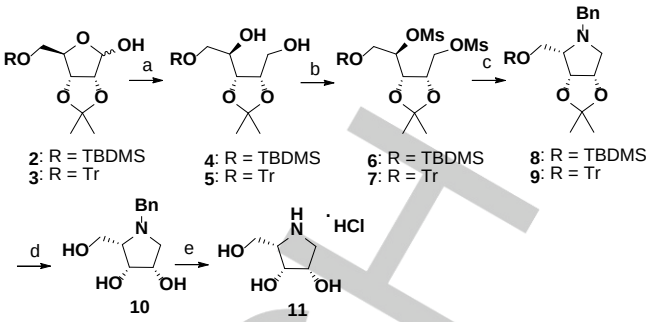

Scheme 1. Synthesis of the pyrrolidines **10** and **11**. *Reagents and conditions:* a) $NaBH_4$, EtOH, rt, 2 h, 90% for **4**, 98% for **5**; b) MsCl, Et_3N, CH_2Cl_2, rt, overnight, 98% for **6**, 95% for **7**; c) $BnNH_2$, 120 °C, 7-8 h, 87% for **8**, 97% for **9**; d) 6M HCl/MeOH 1:2 (v/v), rt, overnight, 62% from **8**, 68% from **9**; e) 1. H_2, 10% Pd-C, MeOH, rt, overnight, 2. 10% HCl, 89%.

$NaBH_4$ was performed in EtOH providing corresponding diols **4**[20] and **5**. Standard mesylation of diols **4** and **5** led smoothly to dimesylated derivatives **6**[20] and **7**. The cyclization of the dimesylate **6** with benzyl amine to access fully protected 1,4-imino-L-lyxitol **8** was conducted previously in refluxing toluene within 24 h.[20] Another substrate very similar to **7** was cyclized to 1,4-imino-L-lyxitol in neat benzyl amine under reflux for 18 h.[21] However, optimization of reaction conditions showed that optimal reaction time and temperature for the cyclization of dimesylates **6** and **7** in neat benzyl amine were 7 h at 120 °C. In addition, the work-up procedure was significantly simplified by extraction of excess $BnNH_2$ with cold 0.5M citric acid[22] instead of its tedious removal by evaporation. Acid-sensitive protective groups were stable under the condition used and the ring closures were performed on a gram scale (~ 3.5 g, yield 87%). Simultaneous removal of isopropylidene and trityl/silyl protective groups from **9** under acidic conditions (6M HCl/MeOH) afforded *N*-benzyl pyrrolidine **10** in moderate yield. In addition, debenzylation of **10** under catalytic hydrogenation conditions followed by treatment with diluted HCl provided the core pyrrolidine **11**[21] as its hydrochloride (Scheme 1).

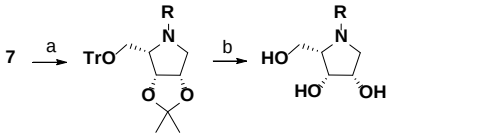

Scheme 2. Synthesis of target pyrrolidines **15**-**17**. *Reagents and conditions:* a) RNH_2, 120 °C, 7-8 h, 87% for **12**, 78% for **13**, 77% for **14**; b) 6M HCl/MeOH 1:2 (v/v), rt, overnight, 52% for **15**, 54% for **16**, 62% for **17**.

Following the optimized conditions for the cyclization reaction, pyrrolidines **12-14** were prepared from dimesylate **7** and the corresponding benzyl amine. Simultaneous hydrolysis of trityl and acetonide protecting group furnished target pyrrolidines **15**-**17** in moderate yields (Scheme 2).

Another approach based on the removal of *N*-benzyl group from **8** under standard conditions (H_2, Pd/C in methanol) followed by *N*-benzylation of the resulting pyrrolidine **18** with *p*-iodo- or *p*-bromobenzyl bromide gave pyrrolidine **19** and **20** in 89% and 74% yield, respectively. Their treatment with 6M HCl in methanol afforded target pyrrolidines **21** and **22** (Scheme 3).

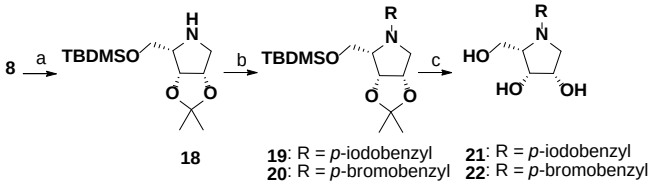

Scheme 3. Synthesis of target pyrrolidines **21** and **22**. *Reagents and conditions:* a) H_2, 10% Pd-C, MeOH, rt, 4 h, 80%; b) RBr, K_2CO_3, DMF, 40 °C, 4h, 89% for **19**, 74% for **20**; c) 6M HCl/MeOH 1:2 (v/v), rt, overnight, 73% for **21**, 66% for **22**.

Biological assays

A series of seven polyhydroxylated pyrrolidines **10**, **11**, **15-17**, **21** and **22** was evaluated towards the class II α-mannosidases (GH family 38) GMIIb, LManII and JBMan and the class I α-mannosidases (GH family 47) AspMan. All *N*-substituted pyrrolidines showed inhibitory activity towards the target enzyme, GMIIb, with IC_{50} values in the range from 52 μM to 770 μM (Table 1).

However, unsubstituted pyrrolidine **11** exhibited only moderate inhibitory activity (IC_{50} = 270 μM). Among the *N*-alkylated pyrrolidines, phenethyl derivative **15** and pyridin-4-ylmethyl derivative **17** were found to be the least potent inhibitors in comparison with *N*-(4-substituted benzyl) analogues **10**, **16**, **21** and **22**. The latter two *N*-(4-halobenzyl)pyrrolidines **21** and **22** were the most potent GMIIb inhibitors with IC_{50} values 52 and 55 μM, respectively. These data suggest that *N*-alkylation plays an important role in the inhibitory activity of the *N*-substituted polyhydroxylated pyrrolidines. For the compounds **10**, **21** and **22** with the lowest IC_{50} values, their inhibition constants were also determined (Table 1). It was observed that K_i values were essentially the same as IC_{50} values, not differing more than by 10%.

A selective GMII inhibitor is required to exhibit none or significantly reduced inhibitory activity towards LMan. All tested polyhydroxylated pyrrolidines were found to be weak LManII inhibitors with IC_{50} values at the millimolar level (IC_{50} in range of 1.2 mM to >8mM). *N*-Substituted derivatives were slightly weaker inhibitors of LManII in comparison with the parent pyrrolidine **11**. It is noteworthy that *N*-phenethyl derivative **15** showed approximately 3-fold higher inhibition capacity than **11**, suggesting that two-carbon spacer between pyrrolidine and benzene ring is a preferred arrangement for LManII inhibition. Thus, it is not the suitable structural fragment of an effective GMIIb inhibitor.

Based on the IC_{50} values for LManII and GMIIb, a selectivity index was calculated for each derivative as a ratio of IC_{50}(LManII)/IC_{50}(GMIIb). The most potent inhibitors of GMIIb **21** and **22** had the highest selectivity index 117 and 136, respectively. *N*-Benzyl pyrrolidine **10** exhibited a slightly lower index of 80. To the best of our knowledge, these structures are the first known GH38 inhibitors with the significantly high selectivity index since all known GH38 inhibitors had the selectivity index <20 (for some example see **23**, **25** and **26** in Table 1) insufficient for clinical treatments. The selectivity index of **16** was also satisfactory and higher than that of the weakest GMIIb inhibitors **17** and **11**. On the contrary, the significantly reduced selectivity was observed for *N*-phenethyl derivative **15**. It seems that a length of hydrocarbon chain between pyrrolidine unit and phenyl function is a crucial factor for retaining the selectivity of the GMIIb inhibitors. The similar inhibitory properties were also observed in our previous study with sulfur-containing α-D-mannopyranosides having the phenylalkyl functional group.[9p]

As published previously [5f] swainsonine **1**, the nanomolar inhibitor of both GMII and LMan, gave an extremely poor selectivity index of 2. A substitution at the position 5 in its analogue **23** led to an increase in the selectivity index to a value of 11. However, a swainsonine derivative with the benzyl functional group itself at the position 5, which could mimic the inhibitor **10** with the high selectivity index, is yet to be described. For such a structure another increase of the selectivity index could be expected to maintain its potency at the nanomolar level. The core structure of the pyrrolidine inhibitors presented here is closely related to the structure of natural 1,4-dideoxy-1,4-imino-D-mannitol **24**, namely its *N*-benzyl derivative **25** (Table 1). When the potency and selectivity of **24** is compared to the inhibitor **11**, the deletion of $-CH(OH)-CH_2OH$ moiety in **24** and the additional attachment of $-CH_2OH$ at the opposite site of the ring in **11** led to a dramatic decrease in potency towards LManII (from 13 μM to 7500 μM) and only to a slight decrease in potency towards GMIIb (from 100 μM to 270 μM) resulting to the required selectivity index. Similarly, when the potency and selectivity of the *N*-benzyl derivatives **25** and the inhibitor **10** are compared, the benzyl function further improved the potency and selectivity (in case of **10**) and only the selectivity (in case of **25**). These results suggest that a combination of an appropriate stereo configuration of $-CH_2OH$ and benzyl functional groups on a mannose mimicking core (polyhydroxylated pyrrolidine ring) may lead to an inhibitor with the required selectivity for the active site of GMIIb.

To verify the high selectivity index and weak inhibitory properties of our pyrrolidine series towards LManII, the inhibition assay was also measured with the α-mannosidase from *Canavalia ensiformis* (Jack bean) (JBMan) (EC 3.2.1.24, GH family 38), widely used as a model for acidic α-mannosides.[2b, 5f, 9e, 9q-r,10, 12a-b] This assay provided similar results as compared to LManII (Table 1). All tested structures did not inhibit JBMan at the 2mM concentration of the inhibitor except for **24**. These results further support the validity of the selectivity index of the *N*-benzyl polyhydroxylated pyrrolidines. Since it is known[2b] that **24** and its pyrrolidine analogues are also strong inhibitors of class I α-mannosidases, further verification of the selectivity index of our compounds (**10**, **11**, **16**, **21**, **22**) towards GMIIb was performed in an enzymatic assay with *Aspergillus saitoi* α-1,2-mannosidase (AspMan) (EC 3.2.1.113, GH family 47). All tested structures, except for unsubstituted derivative **11** (IC_{50} = 1 mM), did not inhibit AspMan at the 1-2 mM concentration of the inhibitor. These results indicate that the most selective inhibitors (**10** and **21**) may maintain their specificity towards Golgi α-mannosidases with no inhibitory effects towards acidic lysosomal and endoplasmic reticulum α-mannosidases. Since the employed model GMIIb from fruit fly showed some distinct biochemical differences in comparison to mannosidase III or mannosidase II[x] from other invertebrates and vertebrates,[15]

Table 1. Measured IC_{50} (and K_i) values [M] for class II (GMIIb, LManII and JBMan) and class I (AspMan) α-mannosidases (in M). For comparison representative inhibitors with a known selectivity index to GMII (as appropriate to either GMII, dGMII or GMIIb) are also included.[6a, 6e, 6r]

Compound	GMIIb IC_{50} [K_i]	LManII IC_{50} (Inhibition in %)[a]	JBMan IC_{50} (Inhibition in %)[a]	AspMan IC_{50} (Inhibition in %)[b]	Selectivity index IC_{50}(LManII)/IC_{50} (GMIIb)
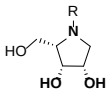					
11	$(2.7 \pm 0.75) \times 10^{-4}$	7.5×10^{-3}	0.7×10^{-3}	$(1.0 \pm 0.2) \times 10^{-3}$	28
(R = H)	[$(2.2 \pm 0.15) \times 10^{-4}$]			(50)	
10	$(8.8 \pm 0.06) \times 10^{-5}$	7.0×10^{-3}	n.d.	n.i.	80
(R = Bn)	[$(7.6 \pm 0.13) \times 10^{-5}$)]		(1)		
15	$(1.9 \pm 0.23) \times 10^{-4}$	1.2×10^{-3}	2.7×10^{-3}	n.m.	6
(R = EtPh)	(n.d.)				
16	$(1.4 \pm 0.17) \times 10^{-4}$	n.d.	n.d.	n.i.	n.d.
(R= 4-MeO-Bn)	(n.d.)	(9)	(4)		
17	$(7.7 \pm 0.40) \times 10^{-4}$	n.d.	n.d.	n.m.	n.d.
(R = 4-Py-Bn)	[n.d.]	(2)	(9)		
21	$(5.2 \pm 0.12) \times 10^{-5}$	6.1×10^{-3}	n.d.	n.i.	117
(R = 4-I-Bn)	[$(5.0 \pm 0.12) \times 10^{-5}$]	(19)	(9)		
22	$(5.5 \pm 0.15) \times 10^{-5}$	7.5×10^{-3}	n.d.	n.i.	136
(R = 4-Br-Bn)	[$(5.8 \pm 0.06) \times 10^{-5}$]	(16)	(8)		
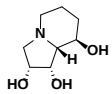	5.0×10^{-8} [c] [3×10^{-9}][d]	11.0×10^{-8} [c]	2.0×10^{-7} [c]	$>10.0 \times 10^{-3}$ [h]	2
1					
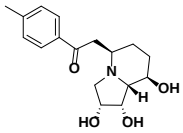	2.9×10^{-8} [d]	3.1×10^{-7} [d]	2.5×10^{-7} [d]	n.m.	11
23					
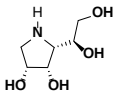	1.0×10^{-4} [e]	1.3×10^{-5} [e]	n.m.	n.m.	<0
24					
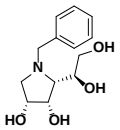	6.9×10^{-4} [e,f]	1.5×10^{-3} [e,f]	n.m.	n.m.	2
25					
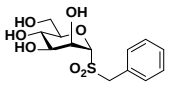	2.0×10^{-3} [g]	n.i.[g]	2.0×10^{-3} [c]	n.i. [b,c]	>2
26					

n.m. - not measured. n.d. - not determined (the inhibition <50% at 8 mM). n.i. - no inhibition or inhibition <10% at 2 mM. [a] inhibition in the presence of 2 mM of the inhibitor calculated towards control activity without inhibitor. [b] inhibition in the presence of 1 mM of the inhibitor calculated towards control activity without inhibitor. [c] IC_{50} values measured for GMIIb, LManII, JBMan and AspMan by Poláková et al.[9q] [d] IC_{50} values measured for dGMII, dLMan and JBMan by Kuntz et al.[5f] [e] IC_{50} values measured for GMII and LMan by Winchester et al. [9a] [f] calculated IC_{50} values by Bobovská et al.[18] based on measured in vitro assays with human α-mannosidases. [9a] [g] IC_{50} values measured for GMIIb and LManII by Poláková et al.[9p] [h] K_i value measured for hERManI by Vallée et al.[23]

additional enzymatic assays with Co^{2+} independent forms of Golgi mannosidase II, GMII, are required for any future refinements of inhibitor design.

Compounds **1**, **10**, **15**, **16**, **21**, **22** were tested *in vitro* for their cytotoxic activity on an eight cancer cell lines: A549 (human lung adenocarcinoma), CCRF-CEM (T-lymphoblastic leukemia), CEM-DNR (T-lymphoblastic leukemia, daunorubicin resistant overexpressing the LRP protein), K562 (acute myeloid leukemia), K562-TAX (acute myeloid leukemia, overexpressing the P-glycoprotein), HCT116 (human

Table 2. Cytotoxic activity of the selected pyrrolidines **10**, **15**, **16**, **21**, **22** and swainsonine **1** against eight tumor and two non-malignant cell lines (IC_{50} in μM).

Comp	A549	CCRF-CEM	CEM-DNR	K562	K562-TAX	HCT116	HCT116p53-/-	U2OS	BJ	MRC-5
10	> 200	101 ± 12	93 ± 11	194 ± 8	107 ± 13	> 200	> 200	> 200	> 200	> 200
15	> 200	95 ± 7	99 ± 11	189 ± 12	117 ± 13	> 200	> 200	> 200	> 200	> 200
16	> 200	105 ± 12	94 ± 10	192 ± 9	110 ± 11	> 200	> 200	200 ± 0.3	> 200	> 200
21	> 200	102 ± 11	87 ± 11	156 ± 10	103 ± 13	> 200	> 200	169 ± 21	> 200	> 200
22	> 200	94 ± 24	122 ± 22	> 200	125 ± 13	> 200	> 200	189 ± 18	> 200	> 200
1	> 200	113 ± 12	132 ± 20	> 200	137 ± 13	> 200	> 200	> 200	> 200	> 200

IC_{50} is the lowest concentration that kills 50 % of cells. The standard deviation in cytotoxicity assays is typically up to 15 % of the average value. Compounds with IC_{50} > 200 μM are considered inactive.

colorectal cancer with wild-type p53), HCT116p53-/- (human colorectal cancer with deleted p53), U2OS (Human Bone Osteosarcoma Epithelial Cells) and on the two non-malignant cell lines BJ (human fibroblast) and MRC-5 (human lung fibroblasts). Cytotoxic activities are presented in Table 2.

In general, cytotoxic activities were observed in high concentrations, and none of the tested compounds were cytotoxic to the non-malignant cell lines BJ and MRC, and solid tumor cell lines HCT116, HTC116p53-/- and A549. In opposite, all compounds were cytotoxic to chemosensitive CCRM-CEM acute lymphoblastic cell line as well as resistant line CEM-DNR with IC_{50} in range of 87-132 μM. The pyrrolidines **10**, **16** a **21** showed slightly higher cytotoxicity for CEM-DNR compared to the non-resistant CCRF-CEM. A similar trend was also observed for the cell line K562 and its resistant counterpart K562-TAX. In addition, pyrrolidine **22** and swainsonine **1** did not inhibit non-resistant K562 at all. The tested *N*-substituted pyrrolidines showed slightly higher cytotoxicity as swainsonine **1** (90 – 130 μM *versus* 110 – 140 μM) indicating that the pyrrolidine structures and the standard **1** may have similar pharmacokinetics properties.

Molecular modeling

The main goals of molecular modeling were to design of a selective GMII inhibitor, and to explain observed selective binding to GMII of the synthesized polyhydroxypyrrolidines. In proposals of new inhibitors computational design was combined with available experimental data of known GH38 inhibitors. We knew from our previous studies [9p, 9r] that appropriate attachment of the benzyl functional group and deletion of 6-hydroxy group on the mannose core of the inhibitor increased selectivity of the inhibitors towards GMIIb. Because the mannoside inhibitors showed only a weak inhibition at the millimolar level, a new core structure of the selective inhibitor had to be designed. The polyhydroxypyrrolidine ring was selected based on structural analogy with α-mannosidase inhibitors swainsonine and 1,4-dideoxy-1,4-imino-D-mannitol. Positions and stereo configurations of functional groups (hydroxy, hydroxylmethyl and benzyl) were optimized by molecular docking. The proposed structures (compounds **10**, **21** and **22)** were further refined by QSAR models with quantum mechanics interaction energy descriptors developed in our laboratory.[18] Other compounds (**11** and **15**-**17**) synthesized in this paper were not proposed by molecular modeling. They were prepared to compare their potency and selectivity with the proposed structures **10**, **21** and **22** as well as to understand an interaction pattern for selective binding to GMIIb of the proposed inhibitors.

To understand the observed selectivity towards GMIIb of the polyhydroxypyrrolidines we focused on two factors which would influence differential binding of inhibitors to GMIIb and LManII (with GMII and LMan as surrogates with known 3D structures); i) possible different ionization states of amino group of the inhibitors and active-site amino acids; and ii) quantum mechanics effects between the inhibitor and active-site amino acids of the enzyme. For this purposes pK_a calculations in water and in both enzymes, docking, hybrid QM/MM geometry optimizations and interaction energy FMO-PIEDA calculations were performed.

pK_a calculations. Polyhydroxypyrrolidines contain an amino functional group incorporated in a ring moiety of the inhibitor. The pK_a values of such amino group may range from 5 to 9 depending on the position of the nitrogen atom in the ring as well as on other structural factors (number and position of hydroxyl groups in the ring, the conformation of the ring, chemical external environment of the amino group, etc.).[24] pH of GMII in Golgi apparatus is about 6 while pH of LMan is more acidic (4.5-5.0) (for more details about pH of enzymatic assays see the section 4.2. Enzyme assays). Thus, inhibitors with a pK_a value of 5-6 units could bind to GMII in neutral form (as an amine) and to LMan in ionized form (as an ammonium cation). This could induce different interaction strength and binding mode as was proposed recently.[13] The calculated pK_a values of the synthesized inhibitors in aqueous solution and in both enzymes are compiled in the Table 3.

The values in aqueous solution are close to a value of 7 being in the range from 6.3-7.9. This indicates that some inhibitors may prefer protonated form and some neutral ones in aqueous solution. For comparison, there are also pK_a value

calculated[13] for swainsonine **1** and pyrrolidine **24**, for which also experimental pK_a value are available.[24a] In the case of dGMII, the inhibitors prefer protonated forms except for **11**, **1** and **24**. In contrast, for the 'acidic' bLMan, all inhibitors prefer protonated forms with pK_a values being in the range from 5.9 to 8.2. In case of the neutral form of the inhibitors the catalytic acid Asp341 in dGMII (and Asp319 in bLMan) is in direct contact with the inhibitor, the neutral (–COOH) form would also be favoured, while for the protonated form of the inhibitors, the ionized form (–COO^-) of this Asp residue is preferred. Interestingly, the adjacent Asp340 residue in dGMII (Ser318 in bLMan) changed its pK_a value depending on the protonation states of Asp341 and the inhibitor. Although these results do not explain a connection between measured IC_{50} of the inhibitors and their protonation states, pK_a calculations clearly indicate that in the active sites, namely in dGMII, there is a balance between protonation states of the inhibitor and some active-site ionizable amino acids. This balance may vary between inhibitors and be dependent on the binding mode, thereby influencing the potency and observed selectivity of the pyrrolidine inhibitors synthesized in this study.

Table 3. Calculated pK_a values for ligands and selected Asp residues in water and in the enzymes.

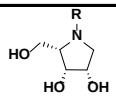

	pK_a					
	Water pH=7		dGMII pH=5.9		bLMan pH=4.5	
Compound	ligand	ligand	Asp341	Asp340	ligand	Asp319
11 (R=H)	7.9	5.9	2.2	5.8	6.9	2.1
10 (R=Bn)	6.3	7.3	2.4	5.9	7.5	2.2
15 (R=EtPh)	6.9	6.8	4.4	4.4	7.8	2.0
16 (R=4-MeO-Bn)	7.5	7.3	2.5	5.9	7.7	2.2
17 (R=4-Py-Bn)	6.4	7.5	2.3	5.9	7.5	1.8
21 (R=4-I-Bn)	6.9	7.4	2.4	5.9	7.3	2.3
22 (R=4-Br-Bn)	7.3	7.3	2.5	5.9	7.3	2.3
1	7.8 [a] (7.5)[b]	5.0 [a]	5.6	4.3	8.2	3.0
24	6.6 [a] (7.4)[b]	4.7 [a]	6.8	4.4	8.1	1.9
Holoenzyme			5.8			3.9

[a] calculated pK_a value by Sladek et al.[13] [b] experimentally measured pK_a values.[2a, 9b]

Molecular docking. By molecular docking it was found that polyhydroxypyrrolidines bind to the active site of both dGMII and bLMan in a similar manner as swainsonine (Figure 1). However, the pyrrolidine ring of our compounds is shifted away from Asp204 and the Zn^{2+} ion as compared to the indolizidine ring of the swainsonine. In Figure 1a there is in superposition of the bound swainsonine (from the crystal structure with ID PDB: 3BLB[5f, 17]) with the computationally

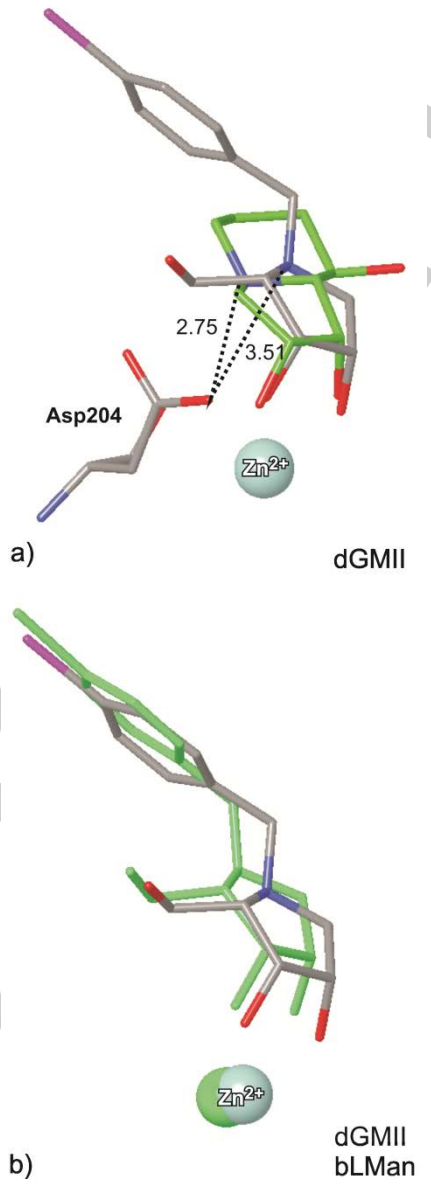

Figure 1. (a) A superposition of the bound swainsonine (PDB ID: 3BLB) [5f, 17] and computationally docked compound **21** into the active site of dGMII. Due to a steric effect of hydroxymethyl moiety of **21** its pyrrolidine ring (in grey) is shift away from the catalytic nucleophile Asp204 compared with the swainsonine ring (in green) (distances between oxygen of Asp204 and nitrogen of the inhibitors are in Å). (b) A superposition of the docked compound **21** in the active site of dGMII (PDB ID: 3BLB)[5f, 17] (**21** with carbons in grey) and bLMan (PDB ID: 1O7D)[8a] (**21** with carbons in green) indicates similar binding mode of both the pyrrolidine core and the benzyl linker.

docked compound **21** in the active site of dGMII. Probably due to a steric effect of hydroxymethyl moiety of **21**, its pyrrolidine ring may not bind so tightly to the bottom of the active site. For example, the distances between the oxygen of Asp204 and the ring nitrogen of the inhibitors are 2.75 Å (for swainsonine) and 3.51 Å (for **21**). The different position of the

amino groups of both analyzed inhibitors may induce different interactions with the active-site residues, namely with Asp204, Asp341 and Zn^{2+}, and influences binding affinities and pK_a values of the pyrrolidine inhibitors.

A superposition of the docked compound **21** in the active site of GMII and bLMan clearly indicates the similar binding mode of both pyrrolidine and benzyl moieties (Figure 1b).

FMO – PIEDA binding analysis. The molecular system under study via the FMO method consisted of 24 fragments including the ligand and the structural water which is always present in the dGMII cavity[5f] for these ligands (for more details see the Experimental section - Molecular modeling). Each fragment corresponded to one of the following amino acids residues: His90, Asp92$^-$, Trp95, Asp204$^-$, Phe206, Arg228$^+$, Tyr267, Ser268, Tyr269, Asp270$^-$, Asp340$^-$, Asp341, Tyr407, Asp409$^-$, Trp415, His470, His471, Asp472$^-$, Tyr727, Arg876$^+$, Gly877, H_2O, Zn^{2+}, and the ligand. Since, as discussed earlier, the main source of GH38 specificity is expected to result from the different binding of the substituent groups attached on the pyrrolidine core. It therefore appears useful to point out residues of the binding site that interact with different parts of the pharmacophores. Firstly, the core structure which is essentially identical to the unsubstituted ligand **11** interacts predominantly with the charge negative residues Asp92, Asp204, Asp472, the charge neutral Tyr727 and Phe206 and the charge positive Zn^{2+} ion. Secondly, more specifically, the interaction of the side-chain –CH_2-OH, which is present also in **11**, is mediated through Asp341, Tyr269 and Asp340. Lastly, the residues in direct interaction with the benzyl linker are Arg228, Arg876, H_2O, Trp415 and Tyr267.

The strongest attractive forces (energies) stem from the Coulomb electrostatic interactions with charged residues. The E_{es} is around −90 to −150 kcal mol^{-1} between the ligand and Asp92 and Asp204. E_{es} is below −150 to −220 kcal mol^{-1} for the interaction with Asp472. This observation is in good qualitative and quantitative agreement with the results for swainsonine by Sladek et al.[13] It is noteworthy that the interaction with Asp204 is considerably weakened if substituents are introduced into the unsubstituted structure **11** (Table S1 of Supplementary data). E_{es} drops from about −156 kcal mol^{-1} in **11** to some −90 to −110 kcal mol^{-1} for the substituted derivatives. Furthermore, the charge transfer + polarisation term E_{ct+mix} of all studied ligands is the largest for **11**. Both may be easily rationalised if one considers the difference in the Asp204···NH-ligand separation being ~1.6 Å for **11** and ~2.5 Å for the remaining ligands. It is due to the steric hindrance of the bulky substituent groups that prevent the ligand from approaching Asp204 much closer.

The main repulsive contribution is from the charge positive Arg228 and Arg876 with E_{es} around 50 and 30 kcal mol^{-1}, respectively. Zn^{2+} is a special case - its total interaction with the ligand is also repulsive. However, it is due to the exchange energy term E_{ex} rather than E_{es}. This can also be interpreted in the same way as for swainsonine,[13] since the interaction with the diol group on the ligand appears to be essential for successful binding in the enzyme. Even though Arg228 and Arg876 are in Coulomb repulsion with the ligand, the benzyl ring exhibits non-negligible dispersion interactions with both residues, which we believe to be important in the stabilization within the enzyme cavity. The E_{disp} with Tyr269 is in all cases around −5 kcal mol^{-1}, which is somewhat more that for swainsonine[13]. Similarly, E_{disp} interaction of **11** with Phe206 is stronger than for swainsonine with some −15 kcal mol^{-1}. The remaining ligands show E_{disp} interaction with Phe206 around −6 to −9 kcal mol^{-1}. The largest E_{disp} originates in the interaction with Trp95 with some −30 to −40 kcal mol^{-1}.

Conclusions

Using available experimental data and computational modeling the structures of the selective inhibitor of fruit fly Golgi α-mannosidase IIb with minimal side-effects towards fruit fly lysosomal α-mannosidase II were designed, synthesized and tested in enzyme and *in vitro* cell line assays. It was found that two functional groups, namely benzyl and hydroxymethyl functions in appropriate stereo configurations, at the core ring of the inhibitor can dictate potency and different binding to the target and side-effect enzymes. It can be concluded that *N*-benzylation of the core polyhydroxylated pyrrolidine unit leads to increased IC_{50} (and K_i) as well as a selectivity index towards GMIIb about 3-fold in comparison with the non-substituted **11**. Further increasing of the potency and the selectivity index can be reached by appropriate substitution at the position 4 on the benzene ring where **21** and **22** had the significant selectivity index >100. Compared with known GMII, dGMII and GMIIb inhibitors, as natural swainsonine (**1**) or 1,4-dideoxy-1,4-imino-D-mannitol (**24**), the structures **10**, **21** and **22** are the first known selective GMIIb inhibitors with minimal side effect towards the lysosomal α-mannosidase II. Since their potency is several orders of magnitude lower than that of swainsonine, further structural refinements will be required to obtain the selective and sufficiently potent inhibitor. Also, additional enzymatic assays with human GMII will be necessary to validate the high selectivity index found for **10**, **21** and **22** in assays with GMIIb. The observed cytotoxic activity of the tested compounds in 72-hour MTS assay is rather low, demonstrating low toxicity on non-tumor cell lines, on the other side is hard to predict its real antitumor potential by the simple cytotoxic test. Such activity should be more likely monitored by synergistic assay with conventional antitumor drugs as doxorubicin, 5-FU or in combination with X-ray irradiation and irinotecan as was published previously for swainsonine and tunicamycin.[25] Experiments with similar design might be a valuable tool in the identification of the real therapeutic potential of GMIIb inhibitors in future.

Based on the results from molecular modeling the potency and the selectivity of the synthesized pyrrolidines might be influenced by the binding position of the pyrrolidine ring (the position of the ring nitrogen to Zn^{2+} and other active-site amino acid residues) and its protonation state giving different interactions with the key active-site residues (Zn^{2+}, Asp341, Asp204, Asp92 and Asp472 in case of dGMII) as was demonstrated in our previous work.[13]

Experimental Section

General chemistry.

TLC was performed on aluminium sheets precoated with silica gel 60 F_{254} (Merck). Flash column chromatography was carried out on silica gel 60 (0.040-0.060 mm, Merck) with distilled solvents (hexanes, ethyl acetate, chloroform, methanol). Dichloromethane was dried (CaH_2) and distilled before use. All reactions containing sensitive reagents were carried out under an argon atmosphere. ^{1}H NMR and ^{13}C NMR spectra were recorded at 25 ºC with Varian VNMRS 400 MHz, Bruker AVANCE III HD 400 and Bruker AVANCE III HDX 600 spectrometers. Chemical shifts are referenced to either TMS (δ 0.00, $CDCl_3$ for ^{1}H) or HOD (δ 4.87, CD_3OD for ^{1}H), and to internal $CDCl_3$ (δ 77.00) or CD_3OD (δ 49.00) for ^{13}C. Optical rotations were measured on a Jasco P2000 polarimeter at 20 °C. High resolution mass determination was performed by ESI-MS on a Thermo Scientific Orbitrap Exactive instrument operating in positive mode.

The lyxitols **10**, **11, 15**, **16**, **17**, **21** and **22** used in biological tests were lyophilized before the use. *p*-Nitrophenyl α-D-mannopyranoside (*p*NP-Man*p*) and jack bean α-mannosidase were purchased from Sigma; swainsonine from Calbiochem; *Aspergillus oryzae* α1,2-mannosidase from Prozyme.

Enzyme assays

Assays with Class II α-Mannosidases (GH family 38). The isolation and purification of recombinant *Drosophila melanogaster* Golgi (GMIIb) and lysosomal (LManII) α-mannosidases was carried out as described by Nemčovičová et al.[15] The α-mannosidase from *Canavalia ensiformis* (Jack bean) (JBMan) was purchased from Sigma. Mannosidase activity of these enzyme preparations were measured using *p*-nitrophenyl-α-D-mannopyranoside (pNP-Man; Sigma; 100 mM stock in dimethylsulphoxide) as a substrate at 2 mM final concentration in 50 mM acetate buffer at the relevant previously-defined optimal pH) (Jack bean α-mannosidase, JBMan, at pH 5.0, GMIIb at pH 6.0, and LManII at pH 5.2) and 0.5 µL of the enzyme (0.05 µg of protein for JBMan), in a total volume of 50 µL for 1-2 h at 37 °C. GMIIb was assayed in the presence of 0.5 mM $CoCl_2$.

The inhibitor was preincubated with the enzyme in the buffer for 5 min at room temperature and the reaction was started by addition of the substrate. The reactions were terminated with two volumes (0.1 mL) of 0.5M sodium carbonate and the production of *p*-nitrophenol was measured at 405 nm using a multimode reader Mithras LB943 (Berthold Technologies).

The average or representative result of three independent experiments made in duplicate is presented. The IC_{50} value was determined with 2 mM *p*NP-Man. The K_i values were determined from Dixon plots of assays performed with *p*NP-Man at the indicated concentration (0.5-4 mM).

Enzyme assays with Class I α-Mannosidase (GH family 47). As *p*NP-Man*p* is not a substrate for GH family 47 enzymes, a MS-based assay was developed using a 2-aminopyridine-labelled $Man_5GlcNAc_2$ *N*-glycan (Manα1,2Manα1,2Manα1,3(Manα1,6)Manβ1,4GlcNAcβ1, 4GlcNAc-PA; purified by RP-HPLC of the *N*-glycome of *Trichomonas vaginalis.*[26] Approximately 5 pmol of the *N*-glycan was incubated with 0.3 µL (4 µU) *Aspergillus saitoi* α1,2-mannosidase in the absence or presence of 0.25-2.0 mM inhibitor, 50 mM ammonium acetate buffer (pH 5) in a total of 5 µL; all assays for 1 or 2 hours at 37 °C. The reactions were heat inactivated for 5 minutes prior to MALDI-TOF MS (Bruker Autoflex Speed); the peak heights of the *m/z* 989, 1151 and 1313 $[M+H]^+$ ions (i.e., corresponding to the substrate and products with one or two α1,2-mannose residues removed) were integrated to estimate the conversion of substrate.

In vitro MTS assays

Cell lines. All cells (if not indicated otherwise) were purchased from the American Tissue Culture Collection (ATCC). The CCRF-CEM line is derived from T lymphoblastic leukemia, evincing high chemosensitivity, K562 represent cells from an acute myeloid leukemia patient sample with bcr-abl translocation, U2OS line is derived from osteosarcoma, HCT116 is colorectal tumor cell line and its p53 gene knock-down counterpart (HCT116p53-/-, Horizon Discovery Ltd, UK) is a model of human cancers with p53 mutation frequently associated with poor prognosis, A549 line is lung adenocarcinoma. The daunorubicin resistant subline of CCRF-CEM cells (CEM-DNR bulk) and paclitaxel-resistant subline K562-TAX were selected in our laboratory by the cultivation of maternal cell lines in increasing concentrations of daunorubicin or paclitaxel, respectively. The CEM-DNR bulk cells overexpress MRP-1 and P-glycoprotein protein, while K562-TAX cells overexpress P-glycoprotein only. Both proteins belong to the family of ABC transporters and are involved in the primary and/or acquired multidrug resistance phenomenon.[27] MRC-5 and BJ cell lines were used as a non-tumor control and represent human fibroblasts. The cells were maintained in nunc/corning 80 cm^2 plastic tissue culture flasks and cultured in cell culture medium according to ATCC or Horizon recommendations (DMEM/RPMI 1640 with 5 g/L glucose, 2 mM glutamine, 100 U/mL penicillin, 100 mg/mL streptomycin, 10% fetal calf serum, and $NaHCO_3$).

Cytotoxic MTS assay. MTS assay was performed at Institute of Molecular and Translational Medicine by robotic platform (HighResBiosolutions). Cell suspensions were prepared and diluted according to the particular cell type and the expected target cell density (25000 – 35000 cells/mL based on cell growth characteristics). Cells were added by automatic pipettor (30 µL) into 384 well microtiter plates. All tested compounds were dissolved in 100% DMSO and four-fold dilutions of the intended test concentration were added in 0.15 µL aliquots at time zero to the microtiter plate wells by the echoacustic non-contact liquid handler Echo550 (Labcyte). The experiments were performed in technical duplicates and three biological replicates at least. The cells were incubated with the tested compounds for 72 h at 37 °C, in a 5% CO_2 atmosphere at 100% humidity. At the end of the incubation period, the cells were assayed by using the MTS test. Aliquots (5 µL) of the MTS stock solution were pipetted into each well and incubated for additional 1–4 h. After this incubation period, the optical density (OD) was measured at 490 nm with an Envision reader (Perkin Elmer). Tumor cell survival (TCS) was calculated by using the following equation: TCS = ($OD_{\text{drug-exposed well}}$/mean $OD_{\text{control wells}}$) × 100%. The IC_{50} value, the drug concentration that is lethal to 50% of the tumor cells, was calculated from the appropriate dose-response curves in Dotmatics software.[27]

Molecular modeling

Docking with Glide. The crystal structures of dGMII (PDB ID: 3BLB),[5f, 17] and bLMan (PDB ID: 1O7D) [8a] were used as 3-D enzyme models of human GMII and LMan for docking of synthesized pyrrolidines with the GLIDE program [28] of the Schrödinger package. Protonation states of amino acid residues of enzymes were calculated for the pH = 6.0 ± 1 (dGMII) and 4.5 ± 1 (bLMan) by the Protein Preparation Wizard of the Schrödinger package.[29] For docking with dGMII all molecules of water at the active site of dGMII were deleted except one (WAT1820, numbering according to PDB ID: 3BLB)[17]. This water has been shown to be conserved in crystal structures of dGMII either with intact substrates or inhibitors.[5f, 9d, 11a] In all docking calculations the catalytic acid (Asp341 in dGMII and Asp319 in the case of (bLMan) was modelled in the protonated form in accordance with its catalytic role as a general acid. The receptor box for the docking conformational search was centred at the Zn^{2+} ion co-factor at the bottom of the active site with a size of 39×39×39 Å using partial atomic charges for the receptor from the OPLS2005 force field except for the Zn^{2+} and side chains of His90, Asp92, Asp204, Arg228, Tyr269, Asp341 and His471 (analogous residues were selected for bLMan). For these structural fragments the charges were calculated at the quantum mechanics level with the DFT (Density Functional Theory) method (M06-2X) [30] using hybrid quantum mechanics/molecular mechanics (QM/MM) model (M06-2X/LACVP**:OPLS2005) with the QSite [31] program of the Schrödinger package. The grid maps were created with no Van der Waals radius and charge scaling for the atoms of the receptor. Flexible docking in standard (SP) precision was used. The partial charges of the ligands were calculated at the DFT level (M06-2X/LACVP**) using the Jaguar program [32] of the

Schrödinger package. The potential for nonpolar parts of the ligands was softened by scaling the Van der Waals radii by a factor of 0.8 for atoms of the ligands with partial atomic charges less than specified cut-off of 0.15. The 5000 poses were kept per ligand for the initial docking stage with scoring window of 100 kcal mol^{-1} for keeping initial poses; the best 400 poses were kept per ligand for energy minimization. The ligand poses with RMS deviations less than 0.5 Å and maximum atomic displacement less than 1.3 Å were discarded as duplicates. The post-docking minimization for 10 ligand poses with the best docking score was performed and optimized structures were saved for subsequent analyses using the MAESTRO [33] viewer of the Schrödinger package.

pK_a calculations. The pK_a values of ligands in water were calculated at the quantum mechanics level, including empirical corrections from the pK_a prediction module[34] of the Jaguar program[32] of the Schrödinger package. pK_a values of ligands bound in the active site of dGMII and bLMan were calculated at the empirical level considering an enzyme pH optimum of 6.0 (dGMII) and 4.5 (bLMan) using the PROPKA v.2 program.[35]

Quantum mechanics calculations. The geometries of complexes (GMII-inhibitor) were optimized at the hybrid QM/MM level using the meta hybrid Minnesota functional with doubled amount of nonlocal exchange (M06-2X) [30] with the Los Alamos national laboratory effective core potential (LACVP**) [36] basis set employing the Qsite program [31b] of the Schrödinger package. The QM part contained ligands, Zn^{2+} and the following active-site amino acids (side chains of His90, Asp92, Trp95, Asp204, Phe206, Arg228, Ser268, Tyr267, Tyr269, Asp270, Asp340, Asp341, Asp409, Trp415, His471, Asp472, Tyr727, Arg876, backbone of Gly877 and WAT1820). The MM part of the system (the rest of the enzyme) was treated with the OPLS2005 force fields.[37] The starting geometries were taken from molecular docking (see the section Docking with Glide).
The virtue of the Fragment Molecular Orbital – Pair Interaction Energy Decomposition Analysis (FMO-PIEDA) technique is to enable evaluation and analysis of pair interactions embedded within the electrostatic potential of the surroundings.[38] This method was successfully used to analyse the change of the binding motif of dGMII ligands when they bind in different protonation states.[13] In this study, we intented to explore its possible use in such way, that individual energy terms could be used in simple QSAR models. That is, to correlate any of the energy terms with experimentally assessed Δ*G* values. The FMO – PIEDA allows the following energy decomposition

$$E_{tot} = E_{els} + E_{exch} + E_{ct\text{-}mix} + E_{disp}$$

Here E_{int} or E_{tot} is the total pair interaction energy, E_{els} is the electrostatic energy, E_{exch} stands for the exchange energy, E_{ct+mix} is the charge-transfer + mixing energy (which is the not fully recovered polarization energy) and E_{disp} is the dispersion energy. E_{exch} is always repulsive as it represents the Pauli exchange term. The electrostatic/Coulomb term can be either positive or negative while the mixing and dispersion terms are negative, thus attractive and stabilizing the interactions. In practice E_{disp} is often used to explain ligand binding in enzymes.[39] We shall focus on E_{int} and E_{disp}. It should be noted that these calculations at the current state of implementation are not corrected for basis set superposition effect (BSSE).[40] Some authors argue this not being a problem at close-to-equilibrium separations of the interacting moieties.[41] General remarks on the FMO accuracy may be found elsewhere.[38b, 42]
FMO-PIEDA analysis was carried out in the GAMESS package [43] using the Def2-SVP basis sets.[44] For each residue (amino acid), its own fragment was assigned and all were in the same layer (i.e. same method applied). The single point calculations were done at the RI-MP2 level.[45] PIEDA background is documented elsewhere.[38a, 46] The HOP – Hybrid Operator Projection technique was adopter in the generation of fragments for the covalently bounded amino acids.[46b] Metal atoms in enzymes represent a challenge for QM description.[47] The approach regarding the zinc atom in dGMII was described earlier.[13]

Acknowledgements

This work was supported by the Slovak Research and Development Agency (the project APVV-0484-12), Scientific Grant Agency of the Ministry of Education of Slovak Republic and Slovak Academy of Sciences (the project VEGA-2/0064/15), the Slovak State Programme Project No. 2003SP200280203 and the Research & Development Operational Programme funded by the ERDF (Amplification of the Centre of Excellence on Green Chemistry Methods and Processes, CEGreenII, Contract No. 26240120025) and the Austrian Science Fund (P29466). The MTS study was supported by grants from the Czech Ministry of Education, Youth and Sports (Grant numbers: LO1304, LM2015063) and IGA-LF-2017-030 (Palacky University). A part of the calculations were performed in the Computing Centre of the Slovak Academy of Sciences using the supercomputing infrastructure acquired in project ITMS 26230120002 and 26210120002 (Slovak infrastructure for high-performance computing) supported by the Research & Development Operational Programme funded by the ERDF.

Keywords: pyrrolidines synthesis • swainsonine • Golgi mannosidase II • cytotoxicity • molecular modeling

References:

[1] S. M. Colegate, P. R. Dorling, C. R. Huxtable, *Aust. J. Chem.* **1979**, *32*, 2257-2264.
[2] a) P. R. Dorling, C. R. Huxtable, S. M. Colegate, *Biochem. J.* **1980**, *191*, 649-651; b) K. W. Moremen, *Biochim. Biophys. Acta, Gen. Subj.* **2002**, *1573*, 225-235; c) D. R. Tulsiani, T. M. Harris, O. Touster, *J. Biol. Chem.* **1982**, *257*, 7936-7939; d) I. Cenci di Dello, P. Dorling, B. Winchester, *Biochem. J.* **1983**, *215*, 693-696; e) D. R. Tulsiani, O. Touster, *Arch. Biochem. Biophys.* **1983**, *224*, 594-600; f) D. R. P. Tulsiani, H. P. Broquist, O. Touster, *Arch. Biochem. Biophys.* **1985**, *236*, 427-434; g) P. E. Goss, M. A. Baker, J. P. Carver, J. W. Dennis, *Clin. Cancer Res.* **1995**, *1*, 935-944.
[3] a) K. Olden, P. Breton, K. Grzegorzewski, Y. Yasuda, B. L. Gause, O. A. Oredipe, S. A. Newton, S. L. White, *Pharmacol. Ther.* **1991**, *50*, 285-290; b) J. W. Dennis, K. Koch, S. Yousefi, I. Vanderelst, *Cancer Res.* **1990**, *50*, 1867-1872.
[4] P. M. Novikoff, O. Touster, A. B. Novikoff, D. P. Tulsiani, *J. Cell Biol.* **1985**, *101*, 339-349.
[5] a) D. R. Rose, *Curr. Opin. Struct. Biol.* **2012**, *22*, 558-562; b) J. M. H. van den Elsen, D. A. Kuntz, D. R. Rose, *EMBO J.* **2001**, *20*, 3008-3017; c) D. R. P. Tulsiani, D. J. Opheim, O. Touster, *J. Biol. Chem.* **1977**, *252*, 3227-3233; d) B. Dewald, O. Touster, *J. Biol. Chem.* **1973**, *248*, 7223-7233; e) K. W. Moremen, O. Touster, P. W. Robbins, *J. Biol. Chem.* **1991**, *266*, 16876-16885; f) D. A. Kuntz, S. Nakayama, K. Shea, H. Hori, Y. Uto, H. Nagasawa, D. R. Rose, *ChemBioChem* **2010**, *11*, 673-680.
[6] D. R. P. Tulsiani, O. Touster, *J. Biol. Chem.* **1983**, *258*, 7578-7585.
[7] a) P. E. Goss, C. L. Reid, D. Bailey, J. W. Dennis, *Clin. Cancer Res.* **1997**, *3*, 1077-1086; b) P. E. Goss, J. Baptiste, B. Fernandes, M. Baker, J. W. Dennis, *Cancer Res.* **1994**, *54*, 1450-1457.
[8] a) P. Heikinheimo, R. Helland, H. K. S. Leiros, I. Leiros, S. Karlsen, G. Evjen, R. Ravelli, G. Schoehn, R. Ruigrok, O. K. Tollersrud, S. McSweeney, E. Hough, *J. Mol. Biol.* **2003**, *327*, 631-644; b) Y. F.

Liao, A. Lal, K. W. Moremen, *J. Biol. Chem.* **1996**, *271*, 28348-28358.

[9] a) B. Winchester, S. Aldaher, N. C. Carpenter, I. C. Dibello, S. S. Choi, A. J. Fairbanks, G. W. J. Fleet, *Biochem. J.* **1993**, *290*, 743-749; b) I. C. Dibello, G. Fleet, S. K. Namgoong, K. Tadano, B. Winchester, *Biochem. J.* **1989**, *259*, 855-861; c) M. Bols, O. Lopez, F. Ortega-Caballero, in *Comprehensive Glycoscience, Vol. 1*, 1st ed. (Ed.: J. P. Kamerling), Elsevier, Oxford, **2007**, pp. 815-867; d) D. A. Kuntz, W. Zhong, J. Guo, D. R. Rose, G. J. Boons, *ChemBioChem* **2009**, *10*, 268-277; e) H. Fiaux, D. A. Kuntz, D. Hoffman, R. C. Janzer, S. Gerber-Lemaire, D. R. Rose, L. Juillerat-Jeanneret, *Bioorg. Med. Chem.* **2008**, *16*, 7337-7346; f) A. Siriwardena, H. Strachan, S. El-Daher, G. Way, B. Winchester, J. Glushka, K. Moremen, G. J. Boons, *ChemBioChem* **2005**, *6*, 845-848; g) B. Li, S. P. Kawatkar, S. George, H. Strachan, R. J. Woods, A. Siriwardena, K. W. Moremen, G. J. Boons, *ChemBioChem* **2004**, *5*, 1220-1227; h) S. George, B. Li, H. Strachan, R. Ayres, R. Collins, A. Siriwardena, K. W. Moremen, G. J. Boons, *Glycobiology* **2002**, *12*, 668-668; i) P. Englebienne, H. Fiaux, D. A. Kuntz, C. R. Corbeil, S. Gerber-Lemaire, D. R. Rose, N. Moitessier, *Proteins* **2007**, *69*, 160-176; j) H. Fiaux, F. Popowycz, S. Favre, C. Schutz, P. Vogel, S. Gerber-Lemaire, L. Juillerat-Jeanneret, *J. Med. Chem.* **2005**, *48*, 4237-4246; k) L. M. Kavlekar, D. A. Kuntz, X. Wen, B. D. Johnston, B. Svensson, D. R. Rose, B. M. Pinto, *Tetrahedron-Asymmetry* **2005**, *16*, 1035-1046; l) D. A. Kuntz, A. Ghavami, B. D. Johnston, B. M. Pinto, D. R. Rose, *Tetrahedron-Asymmetry* **2005**, *16*, 25-32; m) X. Wen, Y. Yuan, D. A. Kuntz, D. R. Rose, B. M. Pinto, *Biochemistry* **2005**, *44*, 6729-6737; n) W. Chen, D. A. Kuntz, T. Hamlet, L. Sim, D. R. Rose, B. M. Pinto, *Bioorg. Med. Chem.* **2006**, *14*, 8332-8340; o) S. P. Kawatkar, D. A. Kuntz, R. J. Woods, D. R. Rose, G. J. Boons, *J. Am. Chem. Soc.* **2006**, *128*, 8310-8319; p) M. Poláková, S. Šesták, E. Lattová, L. Petruš, J. Mucha, I. Tvaroška, J. Kóňa, *Eur. J. Med. Chem.* **2011**, *46*, 944-952; q) M. Poláková, R. Stanton, I. B. H. Wilson, I. Holková, S. Šesták, E. Machová, Z. Jandová, J. Kóňa, *Carbohydr. Res.* **2015**, *406*, 34-40; r) M. Poláková, R. Horák, S. Šesták, I. Holková, *Carbohydr. Res.* **2016**, *428*, 62-71.

[10] a) W. H. Pearson, L. Y. Guo, *Tetrahedron Lett.* **2001**, *42*, 8267-8271; b) E. J. Hembre, W. H. Pearson, *Tetrahedron* **1997**, *53*, 11021-11032; c) R. Shah, J. Carver, J. Marino-Albernas, I. Tvaroška, F. D. Tropper, J. Dennis, in United States Patent Application Publication, US 2003/0236229 A1, GlycoDesign Inc., Toronto (CA), **2003**; d) T. Fujita, H. Nagasawa, Y. Uto, T. Hashimoto, Y. Asakawa, H. Hori, *Org. Lett.* **2004**, *6*, 827-830.

[11] a) N. Shah, D. A. Kuntzt, D. R. Rose, *Proc. Natl. Acad. Sci. U. S. A.* **2008**, *105*, 9570-9575; b) W. Zhong, D. A. Kuntz, B. Ernber, H. Singh, K. W. Moremen, D. R. Rose, G. J. Boons, *J. Am. Chem. Soc.* **2008**, *130*, 8975-8983.

[12] a) Y. Bleriot, T. Dintinger, A. Genregrandpierre, M. Padrines, C. Tellier, *Bioorg. Med. Chem. Lett.* **1995**, *5*, 2655-2660; b) M. P. Heck, S. P. Vincent, B. W. Murray, F. Bellamy, C. H. Wong, C. Mioskowski, *J. Am. Chem. Soc.* **2004**, *126*, 1971-1979; c) D. A. Kuntz, C. A. Tarling, S. G. Withers, D. R. Rose, *Biochemistry* **2008**, *47*, 10058-10068; d) N. S. Kumar, D. A. Kuntz, X. Wen, B. M. Pinto, D. R. Rose, *Proteins* **2008**, *71*, 1484-1496.

[13] V. Sladek, J. Kóňa, H. Tokiwa, *Phys. Chem. Chem. Phys.* **2017**, *19*, 12527-12537.

[14] C. Rabouille, D. A. Kuntz, A. Lockyer, R. Watson, T. Signorelli, D. R. Rose, M. van den Heuvel, D. B. Roberts, *J. Cell Sci.* **1999**, *112*, 3319-3330.

[15] I. Nemčovičová, S. Šesták, D. Rendić, M. Plšková, J. Mucha, I. B. H. Wilson, *Glycoconjugate J.* **2013**, *30*, 899-909.

[16] a) B. S. G. Kumar, G. Pohlentz, M. Schulte, M. Mormann, N. S. Kumar, *Glycobiology* **2014**, *24*, 252-261; b) S. Howard, C. Braun, J. McCarter, K. W. Moremen, Y. F. Liao, S. G. Withers, *Biochem. Biophys. Res. Commun.* **1997**, *238*, 896-898.

[17] D. A. Kuntz, D. R. Rose, Golgi Mannosidase II in complex with swainsonine at 1.3 Angstrom. The Research Collaboratory for Structural Bioinformatics (RCSB): RCSB-Rutgers, RCSB-San Diego Supercomputer Center, and University of Wisconsin-Madison; http://www.rcsb.org. Accessed June 04, 2012; PDB ID: 3BLB.

[18] A. Bobovská, I. Tvaroška, J. Kóňa, *J. Mol. Graph. Model.* **2016**, *66*, 47-57.

[19] a) K. Vamshikrishna, P. Srihari, *Tetrahedron* **2012**, *68*, 1540-1546; b) J. H. Cho, D. L. Bernard, R. W. Sidwell, E. R. Kern, C. K. Chu, *J. Med. Chem.* **2006**, *49*, 1140-1148; c) R. Furst, C. Lentsch, U. Rinner, *Eur. J. Org. Chem.* **2013**, 2293-2297.

[20] D. K. Kim, G. H. Kim, Y. W. Kim, *J. Chem. Soc., Perkin Trans. 1* **1996**, 803-808.

[21] T. B. Mercer, S. F. Jenkinson, B. Bartholomew, R. J. Nash, S. Miyauchi, A. Kato, G. W. J. Fleet, *Tetrahedron-Asymmetry* **2009**, *20*, 2368-2373.

[22] M. Corsi, M. Bonanni, G. Catelani, F. D'Andrea, T. Gragnani, R. Bianchini, *Int. J. Org. Chem.* **2013**, *3*, 41-48.

[23] F. Vallee, P. Yip, F. Lipari, B. Sleno, P. Romero, K. Karaveg, K. Moremen, A. Herscovics, P. L. Howell, *Glycobiology* **2000**, *10*, 1141-1141.

[24] a) G. Legler, in *Inimosugars as Glycosidase Inhibitors: Nojirimycin and beyond* (Ed.: A. E. Stütz), Wiley-VCH Verlag GmbH, Weinheim, **1999**, pp. 31-67; b) O. Lopez, F. L. Qing, C. M. Pedersen, M. Bols, *Bioorg. Med. Chem.* **2013**, *21*, 4755-4761.

[25] J. C. M. De-Freitas-Junior, L. G. Bastos, C. A. Freire-Neto, B. Du Rocher, E. S. F. W. Abdelhay, J. A. Morgado-Diaz, *J. Cell. Biochem.* **2012**, *113*, 2957-296.

[26] K. Paschinger, A. Hykollari, E. Razzazi-Fazeli, P. Greenwell, D. Leitsch, J. Walochnik, I. B. H. Wilson, *Glycobiology* **2012**, *22*, 300-313.

[27] a) V. Nosková, P. Džubák, G. Kuzmina, A. Ludková, D. Stehlik, R. Trojanec, A. Janošťáková, G. Kořínková, V. Mihal, M. Hajduch, *Neoplasma* **2002**, *49*, 418-425; b) P. Perlíková, G. Rylová, P. Nauš, T. Elbert, E. Tloušťová, A. Bourderioux, L. P. Slavětínská, K. Motyka, D. Doležal, P. Znojek, A. Nová, M. Harvanová, P. Džubák, M. Šiller, J. Hlaváč, M. Hajdúch, M. Hocek, *Mol. Cancer Ther.* **2016**, *15*, 922-937.

[28] a) R. A. Friesner, J. L. Banks, R. B. Murphy, T. A. Halgren, J. J. Klicic, D. T. Mainz, M. P. Repasky, E. H. Knoll, M. Shelley, J. K. Perry, D. E. Shaw, P. Francis, P. S. Shenkin, *J. Med. Chem.* **2004**, *47*, 1739-1749; b) Glide, version 7.0, Schrödinger, LLC: New York, NY, 2016.

[29] Schrödinger Suite 2016 Protein Preparation Wizard; Epik v. 3.5; Impact v. 7.0, Schrödinger; Maestro v.10.5, LLC: New York, NY, 2016.

[30] Y. Zhao, D. G. Truhlar, *Theor. Chem. Res.* **2008**, *120*, 215-241.

[31] a) R. B. Murphy, D. M. Philipp, R. A. Friesner, *J. Comput. Chem.* **2000**, *21*, 1442-1457; b) Qsite; Schrödinger, LLC: New York, NY, 2016.

[32] Jaguar, version 9.1, Schrödinger, LLC: New York, NY, 2016.

[33] Maestro, version 10.5; Schrödinger, LLC: New York, NY, 2016.

[34] J. J. Klicic, R. A. Friesner, S. Y. Liu, W. C. Guida, *J. Phys. Chem. A* **2002**, *106*, 1327-1335.

[35] a) H. Li, A. D. Robertson, J. H. Jensen, *Proteins* **2005**, *61*, 704-721; b) D. C. Bas, D. M. Rogers, J. H. Jensen, *Proteins* **2008**, *73*, 765-783.

[36] a) W. R. Wadt, P. J. Hay, *J. Chem. Phys.* **1985**, *82*, 284-298; b) P. J. Hay, W. R. Wadt, *J. Chem. Phys.* **1985**, *82*, 270-283.

[37] G. A. Kaminski, R. A. Friesner, J. Tirado-Rives, W. L. Jorgensen, *J. Phys. Chem. B* **2001**, *105*, 6474-6487.

[38] a) D. G. Fedorov, T. Nagata, K. Kitaura, *Phys. Chem. Chem. Phys.* **2012**, *14*, 7562-7577; b) S. Tanaka, Y. Mochizuki, Y. Komeiji, Y. Okiyama, K. Fukuzawa, *Phys. Chem. Chem. Phys.* **2014**, *16*, 10310-10344; c) D. G. Fedorov, K. Kitaura, *The Fragnemt Molecular Orbital Method - Practical Applications to Large Molecular Systems*, CRC Press, Taylor and Francis Group, **2009**; d) M. S. Gordon, D. G. Fedorov, S. R. Pruitt, L. V. Slipchenko, *Chem. Rev.* **2012**, *112*, 632-672.

[39] a) S. Arulmozhiraja, N. Matsuo, E. Ishitsubo, S. Okazaki, H. Shimano, H. Tokiwa, *PLoS One* **2016**, *11*; b) N. Sriwilaijaroen, S. Magesh, A. Imamura, H. Ando, H. Ishida, M. Sakai, E. Ishitsubo, T.

Hori, S. Moriya, T. Ishikawa, K. Kuwata, T. Odagiri, M. Tashiro, H. Hiramatsu, K. Tsukamoto, T. Miyagi, H. Tokiwa, M. Kiso, Y. Suzuki, *J. Med. Chem.* **2016**, *59*, 4563-4577.

[40] S. F. Boys, F. Bernardi, *Mol. Phys.* **1970**, *19*, 553-566.

[41] X. W. Sheng, L. Mentel, O. V. Gritsenko, E. J. Baerends, *J. Comput. Chem.* **2011**, *32*, 2896-2901.

[42] K. Fukuzawa, C. Watanabe, I. Kurisaki, N. Taguchi, Y. Mochizuki, T. Nakano, S. Tanaka, Y. Komeiji, *Comput. Theor. Chem.* **2014**, *1034*, 7-16.

[43] a) M. W. Schmidt, K. K. Baldridge, J. A. Boatz, S. T. Elbert, M. S. Gordon, J. H. Jensen, S. Koseki, N. Matsunaga, K. A. Nguyen, S. J. Su, T. L. Windus, M. Dupuis, J. A. Montgomery, *J. Comput. Chem.* **1993**, *14*, 1347-1363; b) M. S. Gordon, M. W. Schmidt, *Theory and Applications of Computational Chemistry*, Elsevier, **2005**.

[44] a) F. Weigend, *Phys. Chem. Chem. Phys.* **2006**, *8*, 1057-1065; b) F. Weigend, R. Ahlrichs, *Phys. Chem. Chem. Phys.* **2005**, *7*, 3297-3305.

[45] X. G. Ren, P. Rinke, V. Blum, J. Wieferink, A. Tkatchenko, A. Sanfilippo, K. Reuter, M. Scheffler, *New J. Phys.* **2012**, *14*, 053020.

[46] a) M. C. Green, D. G. Fedorov, K. Kitaura, J. S. Francisco, L. V. Slipchenko, *J. Chem. Phys.* **2013**, *138*; b) D. G. Fedorov, K. Kitaura, *J. Comput. Chem.* **2007**, *28*, 222-237.

[47] V. Sladek, I. Tvaroška, *J. Phys. Chem. B* **2017**, *121*, 6148-6162.

Entry for the Table of Contents

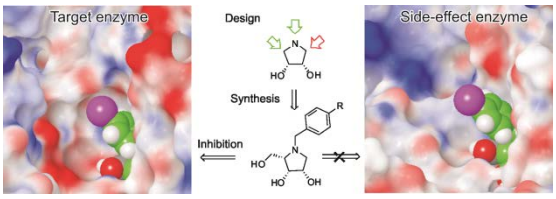

Selective GMIIb inhibitors: The synthesized *N*-benzyl substituted polyhydroxypyrrolidines represent the first known selective inhibitors of Golgi α-mannosidase IIb. The attachment of two functional groups, namely benzyl and hydroxymethyl function in appropriate stereo configuration, at the core ring of the inhibitor can dictate potency and different binding to the target and side-effect enzymes.